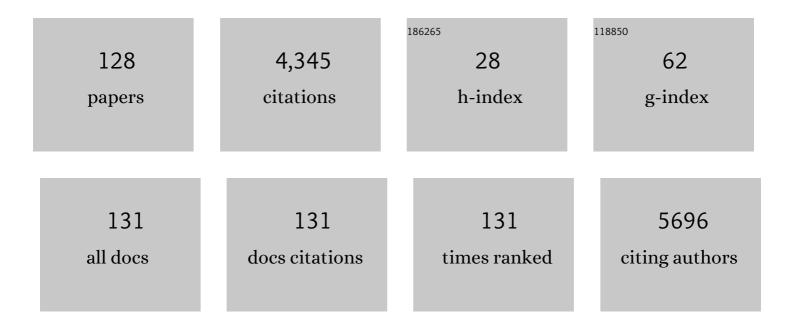
T Jean Daou

List of Publications by Year in descending order

Source: https://exaly.com/author-pdf/7168291/publications.pdf Version: 2024-02-01



Τ ΙΕΛΝ ΠΛΟΙΙ

#	Article	IF	CITATIONS
1	Highly efficient non-microwave instant heating synthesis of hexyl levulinate fuel additive enhanced by sulfated nanosilica catalyst. Microporous and Mesoporous Materials, 2022, 331, 111645.	4.4	6
2	Determination of Microporous and Mesoporous Surface Areas and Volumes of Mesoporous Zeolites by Corrected <i>t</i> â€Plot Analysis. ChemNanoMat, 2022, 8, .	2.8	12
3	SAPO-34 crystallized using novel pyridinium template as highly active catalyst for synthesis of ethyl levulinate biofuel. Microporous and Mesoporous Materials, 2022, 333, 111754.	4.4	3
4	SAPO-35 zeolite crystallized using novel structure-directing agent for catalytic conversion of levulinic acid into ethyl levulinate under non-microwave instant heating. Materials Chemistry and Physics, 2022, 287, 126240.	4.0	3
5	Experimental and numerical investigation of specific behaviour of fluoride ions during filtration of pure salt water solutions with titania membrane. Desalination, 2022, 537, 115870.	8.2	0
6	Rational Design and Characterisation of Novel Mono- and Bimetallic Antibacterial Linde Type A Zeolite Materials. Journal of Functional Biomaterials, 2022, 13, 73.	4.4	4
7	Synthesis of BEC-type germanosilicates with asymmetric diquaternary ammonium salts. Microporous and Mesoporous Materials, 2021, 312, 110804.	4.4	2
8	Facile and fast determination of Si/Al ratio of zeolites using FTIR spectroscopy technique. Microporous and Mesoporous Materials, 2021, 311, 110683.	4.4	47
9	High Quality Bio-Oil Obtained from Catalyzed Pyrolysis of Olive Mill Solid Wastes in a Bi-Functional Reactor. Materials Sciences and Applications, 2021, 12, 52-77.	0.4	1
10	Offretite Zeolite Single Crystals Synthesized by Amphiphile-Templating Approach. Molecules, 2021, 26, 2238.	3.8	0
11	All-Silica SSZ-74 Synthesized in Fluoride or Fluoride-Free Media: Investigation on Organic Structure-Directing Agent's Locations Inside Pores. Crystal Growth and Design, 2021, 21, 4013-4022.	3.0	3
12	Synthesis of Hierarchical MOR-Type Zeolites with Improved Catalytic Properties. Molecules, 2021, 26, 4508.	3.8	4
13	Zeolite-Polymer Composite Materials as Water Scavenger. Molecules, 2021, 26, 4815.	3.8	5
14	Hierarchical Zeolites as Catalysts for Biodiesel Production from Waste Frying Oils to Overcome Mass Transfer Limitations. Molecules, 2021, 26, 4879.	3.8	13
15	A Novel Numerical Procedure to Estimate the Electric Charge in the Pore from Filtration of Single-Salt Solutions. Membranes, 2021, 11, 726.	3.0	2
16	Offretite zeolite templated by amphiphile and its catalytic performance in microwave-assisted Knoevenagel condensation of benzaldehyde and ethyl cyanoacetate. Materials Chemistry and Physics, 2021, 272, 125001.	4.0	4
17	Esterification of linoleic acid using HZSM-5 zeolites with different Si/Al ratios. Microporous and Mesoporous Materials, 2020, 294, 109855.	4.4	20
18	Organic/Inorganic Heterogeneous Silicaâ€Based Photoredox Catalyst for Azaâ€Henry Reactions. European Journal of Organic Chemistry, 2020, 2020, 1572-1578.	2.4	23

#	Article	IF	CITATIONS
19	The effect of nanostructures on high pressure intrusion–extrusion of water and electrolyte solutions in hierarchical nanoboxes of silicalite-1. New Journal of Chemistry, 2020, 44, 273-281.	2.8	7
20	Recyclable synthesis of Cs-ABW zeolite nanocrystals from non-reacted mother liquors with excellent catalytic henry reaction performance. Journal of Environmental Chemical Engineering, 2020, 8, 103579.	6.7	7
21	Guided Crystallization of Zeolite Beads Composed of ZSM-12 Nanosponges. Crystals, 2020, 10, 828.	2.2	1
22	Deposition of NiO Nanoparticles on Nanosized Zeolite NaY for Production of Biofuel via Hydrogen-Free Deoxygenation. Materials, 2020, 13, 3104.	2.9	13
23	Efficient Removal of Volatile Organic Compounds by FAU-Type Zeolite Coatings. Molecules, 2020, 25, 3336.	3.8	5
24	Green hybrid zeolite coatings for on-orbit molecular decontamination. Microporous and Mesoporous Materials, 2020, 307, 110478.	4.4	3
25	Synthesis of FAU-Type Zeolite Membranes with Antimicrobial Activity. Molecules, 2020, 25, 3414.	3.8	10
26	Effect of zeolite morphology on charge separated states: ZSM-5-type nanocrystals, nanosheets and nanosponges. Physical Chemistry Chemical Physics, 2020, 22, 12015-12027.	2.8	3
27	Energetic Performance of Pure Silica Zeolites under High-Pressure Intrusion of LiCl Aqueous Solutions: An Overview. Molecules, 2020, 25, 2145.	3.8	12
28	Controlled Crystallization of Hierarchical Monoliths Composed of Nanozeolites. Crystal Growth and Design, 2020, 20, 5413-5423.	3.0	5
29	Synthesis of Hierarchical Zeolites with Morphology Control: Plain and Hollow Spherical Beads of Silicalite-1 Nanosheets. Molecules, 2020, 25, 2563.	3.8	5
30	Influence of the Compensating Cation Nature on the Water Adsorption Properties of Zeolites. Molecules, 2020, 25, 944.	3.8	31
31	Crystal growth study of nanosized K-MER zeolite from bamboo leaves ash and its catalytic behaviour in Knoevenagel condensation of benzaldehyde with ethyl cyanoacetate. Materials Chemistry and Physics, 2020, 251, 123100.	4.0	5
32	Hierarchical Cs–Pollucite Nanozeolite Modified with Novel Organosilane as an Excellent Solid Base Catalyst for Claisen–Schmidt Condensation of Benzaldehyde and Acetophenone. Processes, 2020, 8, 96.	2.8	7
33	Structural interpretation of the energetic performances of a pure silica LTA-type zeolite. Physical Chemistry Chemical Physics, 2020, 22, 5178-5187.	2.8	11
34	Unusual high-pressure intrusion-extrusion behavior of electrolyte solutions in Mu-26, a pure silica zeolite of topology STF. Microporous and Mesoporous Materials, 2020, 298, 110047.	4.4	7
35	Morphological effects on catalytic performance of LTL zeolites in acylation of 2-methylfuran enhanced by non-microwave instant heating. Materials Chemistry and Physics, 2020, 244, 122688.	4.0	14
36	Ultrasmall Cs-AlMCM-41 basic catalysts: Effects of aluminum addition on their physico-chemical and catalytic properties. Microporous and Mesoporous Materials, 2019, 288, 109599.	4.4	6

#	Article	IF	CITATIONS
37	Reminiscent capillarity in subnanopores. Nature Communications, 2019, 10, 4642.	12.8	33
38	Hierarchical ZSM-5 beads composed of zeolite nanosheets obtained by pseudomorphic transformation. Microporous and Mesoporous Materials, 2019, 288, 109565.	4.4	8
39	Preparation of Single-Crystal "House-of-Cards―like ZSM-5 and Their Performance in Ethanol-to-Hydrocarbon Conversion. Chemistry of Materials, 2019, 31, 4639-4648.	6.7	45
40	Differential penetration of ethanol and water in Si-chabazite: High pressure dehydration of azeotrope solution. Microporous and Mesoporous Materials, 2019, 284, 161-169.	4.4	15
41	Surfactant-modified MFI-type nanozeolites: Super-adsorbents for nitrate removal from contaminated water. Microporous and Mesoporous Materials, 2019, 283, 1-13.	4.4	29
42	High pressure intrusion of water and LiCl aqueous solutions in hydrophobic KIT-6 mesoporous silica: Influence of the grafted group nature. Microporous and Mesoporous Materials, 2019, 280, 248-255.	4.4	20
43	Micro- and macroscopic observations of the nucleation process and crystal growth of nanosized Cs-pollucite in an organotemplate-free hydrosol. New Journal of Chemistry, 2019, 43, 17433-17440.	2.8	9
44	Study on the catalytic performance of different crystal morphologies of HZSM-5 zeolites for the production of biodiesel: a strategy to increase catalyst effectiveness. Catalysis Science and Technology, 2019, 9, 5456-5471.	4.1	21
45	Performance of surfactant-modified *BEA-type zeolite nanosponges for the removal of nitrate in contaminated water: Effect of the external surface. Journal of Hazardous Materials, 2019, 364, 206-217.	12.4	46
46	Synthesis of Cs-ABW nanozeolite in organotemplate-free system. Microporous and Mesoporous Materials, 2019, 277, 78-83.	4.4	22
47	A drastic influence of the anion nature and concentration on high pressure intrusion–extrusion of electrolyte solutions in Silicalite-1. Physical Chemistry Chemical Physics, 2018, 20, 6462-6468.	2.8	11
48	Synthesis of hierarchical ZSM-48 nano-zeolites. New Journal of Chemistry, 2018, 42, 4457-4464.	2.8	12
49	Energetic Performances of Pure-Silica DDR Zeolite by High-Pressure Intrusion–Extrusion of Electrolyte Aqueous Solutions: A Shock-Absorber with Huge Absorbed Energy. Journal of Physical Chemistry C, 2018, 122, 2726-2733.	3.1	14
50	Extra large pore opening CFI and DON-type zeosils for mechanical energy storage. Microporous and Mesoporous Materials, 2018, 255, 211-219.	4.4	11
51	Periodic mesoporous organosilicas as porous matrix for heterogeneous lyophobic systems. Microporous and Mesoporous Materials, 2018, 260, 166-171.	4.4	14
52	Intrusion–Extrusion of Electrolyte Aqueous Solutions in Pure Silica Chabazite by in Situ High Pressure Synchrotron X-ray Powder Diffraction. Journal of Physical Chemistry C, 2018, 122, 28001-28012.	3.1	12
53	Synthesis of Binderless ZK-4 Zeolite Microspheres at High Temperature. Molecules, 2018, 23, 2647.	3.8	9
54	Adsorption of Polychlorinated Aromatics in EMT-Type Zeolites: A Combined Experimental-Simulation Approach. Journal of Physical Chemistry C, 2018, 122, 12731-12741.	3.1	4

T Jean Daou

#	Article	IF	CITATIONS
55	Catalytic properties of Ga-containing MFI-type zeolite in cyclohexane dehydrogenation and propane aromatization. Journal of Catalysis, 2018, 365, 376-390.	6.2	40
56	Exploring the impact of zeolite porous voids in liquid phase reactions: The case of glycerol etherification by tert-butyl alcohol. Journal of Catalysis, 2018, 365, 249-260.	6.2	34
57	Porous sorbents for the capture of radioactive iodine compounds: a review. RSC Advances, 2018, 8, 29248-29273.	3.6	246
58	New Approach to the Acidity Characterization of Pristine Zeolite Crystals by Ethylene Using Reversed-Flow Inverse Gas Chromatography (RF-IGC). Journal of Physical Chemistry C, 2017, 121, 2738-2747.	3.1	2
59	Influence of LiCl aqueous solution concentration on the energetic performances of pure silica chabazite. New Journal of Chemistry, 2017, 41, 2586-2592.	2.8	13
60	Investigation of the energetic performance of pure silica BEC-type zeolite under high pressure water and 20AM LiCl intrusion-extrusion experiments. Microporous and Mesoporous Materials, 2017, 254, 153-159.	4.4	13
61	Adsorption of volatile organic compounds in composite zeolites pellets for space decontamination. Adsorption, 2017, 23, 395-403.	3.0	14
62	SDA-Free Hydrothermal Synthesis of High-Silica Ultra-nanosized Zeolite Y. Crystal Growth and Design, 2017, 17, 1173-1179.	3.0	32
63	Effects of the zeolite particle size on the charge separated states. Microporous and Mesoporous Materials, 2017, 254, 121-127.	4.4	7
64	Energetic performances of FER-type zeolite in the presence of electrolyte solutions under high pressure. Energy, 2017, 130, 29-37.	8.8	8
65	Dioxin and 1,2-dichlorobenzene adsorption in aluminosilicate zeolite Beta. Adsorption, 2017, 23, 101-112.	3.0	8
66	Adsorption of 1,2-dichlorobenzene and 1,2,4-trichlorobenzene in nano- and microsized crystals of MIL-101(Cr): static and dynamic gravimetric studies. Environmental Science and Pollution Research, 2017, 24, 26562-26573.	5.3	12
67	Formation domain of SDA-free Y faujasite small crystals. New Journal of Chemistry, 2017, 41, 13260-13267.	2.8	6
68	Impact of Crystal Size on the Acidity and the Involved Interactions Studied by Conventional and Innovative Techniques. Journal of Physical Chemistry C, 2017, 121, 18725-18737.	3.1	3
69	Heterogeneous lyophobic systems based on pure silica ITH-type zeolites: high pressure intrusion of water and electrolyte solutions. New Journal of Chemistry, 2017, 41, 15087-15093.	2.8	8
70	Adsorption of uremic toxins over dealuminated zeolites. Adsorption Science and Technology, 2017, 35, 3-19.	3.2	20
71	Intrusion–extrusion of electrolytic solutions in zeolites for energy storage. Acta Crystallographica Section A: Foundations and Advances, 2017, 73, C1427-C1427.	0.1	0
72	Prediction of the mechanical properties of zeolite pellets for aerospace molecular decontamination applications. Beilstein Journal of Nanotechnology, 2016, 7, 1761-1771.	2.8	4

#	Article	IF	CITATIONS
73	Eco-compatible zeolite-catalysed continuous halogenation of aromatics. Green Chemistry, 2016, 18, 4714-4724.	9.0	24
74	A new generation of MFI-type zeolite pellets with very high mechanical performance for space decontamination. Microporous and Mesoporous Materials, 2016, 221, 167-174.	4.4	21
75	Intrusion-extrusion experiments of MgCl2 aqueous solution in pure silica ferrierite: Evidence of the nature of intruded liquid by in situ high pressure synchrotron X-ray powder diffraction. Microporous and Mesoporous Materials, 2016, 235, 253-260.	4.4	25
76	Hierarchical Faujasite-Type Zeolite for Molecular Decontamination. Journal of Nanoscience and Nanotechnology, 2016, 16, 9318-9322.	0.9	12
77	Intrusion–extrusion spring performance of –COK-14 zeolite enhanced by structural changes. Physical Chemistry Chemical Physics, 2016, 18, 18795-18801.	2.8	11
78	Influence of downsizing of zeolite crystals on the orthorhombic ↔ monoclinic phase transition in pure silica MFI-type. Solid State Sciences, 2016, 58, 111-114.	3.2	6
79	Particular properties of the coke formed on nano-sponge *BEA zeolite during ethanol-to-hydrocarbons transformation. Journal of Catalysis, 2016, 336, 1-10.	6.2	56
80	New Generation of Zeolite Materials for Environmental Applications Journal of Physical Chemistry C, 2016, 120, 2688-2697.	3.1	32
81	Synthesis of EMT/FAU-type zeolite nanocrystal aggregates in high yield and crystalline form. Comptes Rendus Chimie, 2016, 19, 475-485.	0.5	8
82	Impact of extreme downsizing of *BEA-type zeolite crystals on n-hexadecane hydroisomerization. New Journal of Chemistry, 2016, 40, 4335-4343.	2.8	28
83	Synthesis of mono- and bi-layer zeolite films on alumina substrates. Comptes Rendus Chimie, 2016, 19, 486-495.	0.5	5
84	Elaboration of FAU-type zeolite beads with good mechanical performances for molecular decontamination. RSC Advances, 2016, 6, 2470-2478.	3.6	25
85	High pressure intrusion–extrusion of electrolyte solutions in aluminosilicate FAU and *BEA-type zeolites. Microporous and Mesoporous Materials, 2016, 221, 1-7.	4.4	15
86	Hydraulic Performance Modifications of a Zeolite Membrane after an Alkaline Treatment: Contribution of Polar and Apolar Surface Tension Components. Advances in Materials Science and Engineering, 2015, 2015, 1-7.	1.8	4
87	High-Pressure Intrusion–Extrusion of Water and Electrolyte Solutions in Pure-Silica LTA Zeolite. Journal of Physical Chemistry C, 2015, 119, 28319-28325.	3.1	29
88	One shot synthesis of EMT-type zeolite nanocrystals aggregates for potential industrial applications. Microporous and Mesoporous Materials, 2015, 210, 194-198.	4.4	8
89	The influence of the nature of organosilane surfactants and their concentration on the formation of hierarchical FAU-type zeolite nanosheets. New Journal of Chemistry, 2015, 39, 2675-2681.	2.8	24
90	Synthesis of mono- and bi-layer MFI zeolite films on macroporous alumina tubular supports: Application to nanofiltration. Journal of Crystal Growth, 2015, 428, 71-79.	1.5	10

#	Article	IF	CITATIONS
91	Influence of the Particle Sizes on the Energetic Performances of MFI-Type Zeolites. Journal of Physical Chemistry C, 2015, 119, 18074-18083.	3.1	22
92	Surface energy modification of a Na-mordenite thin layer treated by an alkaline solution. Materials Express, 2015, 5, 451-456.	0.5	7
93	Synthesis of a New Diaazacrown Ether Compound Interconnected with an Azacrown Ether and Decorated with a Long Lipophilic Chain. Synthetic Communications, 2014, 44, 1888-1892.	2.1	0
94	High Pressure Intrusion–Extrusion of LiCl Aqueous Solutions in Silicalite-1 Zeolite: Influence on Energetic Performances. Journal of Physical Chemistry C, 2014, 118, 3935-3941.	3.1	43
95	Influence of the aqueous medium on the energetic performances of Silicalite-1. Materials Letters, 2014, 115, 229-232.	2.6	46
96	Drastic change of the intrusion–extrusion behavior of electrolyte solutions in pure silica *BEA-type zeolite. Physical Chemistry Chemical Physics, 2014, 16, 17893-17899.	2.8	35
97	Synthesis of purely silica MFI-type nanosheets for molecular decontamination. RSC Advances, 2014, 4, 37353.	3.6	35
98	A Comparative Study of Some Properties of Cassava and Tree Cassava Starch Films. Physics Procedia, 2014, 55, 220-226.	1.2	33
99	MFI-type zeolite nanosheets for gas-phase aromatics chlorination: a strategy to overcome mass transfer limitations. RSC Advances, 2014, 4, 27242-27249.	3.6	13
100	Energetic performances of pure silica STF and MTT-type zeolites under high pressure water intrusion. RSC Advances, 2014, 4, 37655-37661.	3.6	27
101	The influence of I-lysine and PDADMA on the crystal size and porosity of zeolite Y material. Microporous and Mesoporous Materials, 2013, 170, 346-351.	4.4	13
102	One-pot structural conversion of magadiite into MFI zeolite nanosheets using mononitrogen surfactants as structure and shape-directing agents. CrystEngComm, 2013, 15, 3009.	2.6	33
103	Synthesis of MFI/EMT zeolite bi-layer films for molecular decontamination. Chemical Engineering Journal, 2013, 234, 66-73.	12.7	21
104	Synthesis of FAU and EMT-type zeolites using structure-directing agents specifically designed by molecular modelling. Microporous and Mesoporous Materials, 2013, 174, 117-125.	4.4	34
105	Energetic behavior of the pure silica ITQ-12 (ITW) zeolite under high pressure water intrusion. Physical Chemistry Chemical Physics, 2013, 15, 20320.	2.8	31
106	Tensile and water barrier properties of cassava starch composite films reinforced by synthetic zeolite and beidellite. Journal of Food Engineering, 2013, 115, 339-346.	5.2	28
107	Gas-phase chlorination of aromatics over FAU- and EMT-type zeolites. Catalysis Communications, 2013, 39, 10-13.	3.3	11
108	Zeolite hybrid films for space decontamination. Microporous and Mesoporous Materials, 2013, 172, 36-43.	4.4	24

#	Article	IF	CITATIONS
109	Adsorption of volatile organic compounds in pure silica CHA, â^—BEA, MFI and STT-type zeolites. Microporous and Mesoporous Materials, 2013, 173, 147-154.	4.4	74
110	MFI/â^—BEA hybrid coating on aluminum alloys. Microporous and Mesoporous Materials, 2013, 166, 79-85.	4.4	18
111	Evaluation and Treatment of Carbonyl Compounds and Fine Particles Emitted by Combustion of Biodiesels in a Generator. Energy & amp; Fuels, 2012, 26, 6160-6167.	5.1	11
112	Key steps influencing the formation of ZSM-5 films on aluminum substrates. Microporous and Mesoporous Materials, 2012, 152, 1-8.	4.4	35
113	Adsorption kinetics and equilibrium of phenol drifts on three zeolites. Open Engineering, 2012, 2, .	1.6	8
114	Surfactant-modified MFI nanosheets: a high capacity anion-exchanger. Chemical Communications, 2011, 47, 902-904.	4.1	36
115	Study of Non-Regulated Exhaust Emissions Using Biodiesels and Impact on a 4 Way Catalyst Efficiency. , 2011, , .		4
116	In vitro and in vivo intracellular delivery of quantum dots by maurocalcine. International Journal of Biomedical Nanoscience and Nanotechnology, 2011, 2, 12.	0.1	6
117	Effect of chain length and electrical charge on properties of ammonium-bearing bisphosphonate-coated superparamagnetic iron oxide nanoparticles: formulation and physicochemical studies. Journal of Nanoparticle Research, 2010, 12, 1239-1248.	1.9	23
118	Spin Canting of Maghemite Studied by NMR and In-Field Mössbauer Spectrometry. Journal of Physical Chemistry C, 2010, 114, 8794-8799.	3.1	43
119	Formation of Ferrimagnetic Films with Functionalized Magnetite Nanoparticles Using the Langmuirâ ^{~,} Blodgett Technique. Journal of Physical Chemistry B, 2009, 113, 734-738.	2.6	22
120	Effect of Poly(ethylene glycol) Length on the in Vivo Behavior of Coated Quantum Dots. Langmuir, 2009, 25, 3040-3044.	3.5	142
121	Water soluble dendronized iron oxide nanoparticles. Dalton Transactions, 2009, , 4442.	3.3	85
122	Thermal, Magnetic, and Luminescent Properties of Dendronized Ferrite Nanoparticles. Journal of Physical Chemistry C, 2009, 113, 12201-12212.	3.1	30
123	Highly Luminescent CuInS ₂ /ZnS Core/Shell Nanocrystals: Cadmium-Free Quantum Dots for In Vivo Imaging. Chemistry of Materials, 2009, 21, 2422-2429.	6.7	644
124	Coupling Agent Effect on Magnetic Properties of Functionalized Magnetite-Based Nanoparticles. Chemistry of Materials, 2008, 20, 5869-5875.	6.7	298
125	Design of Functionalized Fe3O4 Nanoparticles for Elaboration of Nanostructured Films with Magnetic Properties. Materials Research Society Symposia Proceedings, 2007, 1007, 1.	0.1	0
126	Phosphate Adsorption Properties of Magnetite-Based Nanoparticles. Chemistry of Materials, 2007, 19, 4494-4505.	6.7	368

#	Article	IF	CITATIONS
127	Investigation of the grafting rate of organic molecules on the surface of magnetite nanoparticles as a function of the coupling agent. Sensors and Actuators B: Chemical, 2007, 126, 159-162.	7.8	31
128	Hydrothermal Synthesis of Monodisperse Magnetite Nanoparticles. Chemistry of Materials, 2006, 18, 4399-4404.	6.7	558